https://doi.org/10.1016/j.compgeo.2018.07.010

Probabilistic assessment of pile group response considering superstructure stiffness and three-dimensional soil spatial variability

Y.F. Leung*, and M.K. Lo

Department of Civil and Environmental Engineering, The Hong Kong Polytechnic University, Hung Hom, Hong Kong

Abstract

This note presents the probabilistic analyses of pile groups considering spatially variable soil properties and superstructure-foundation interaction effects. Condensed stiffness matrices for the superstructure and spatially variable subsurface domain are evaluated individually, and coupled with foundation elements for holistic analyses of the system. Probabilistic assessments are then performed using surrogate modeling method. Parametric studies show that common assumptions of perfect or no spatial correlations in the soil may not represent the critical scenario for pile groups. Two presented foundation case studies also reveal the significance of interactions between superstructure and soil variability, and potentials of foundation tilting due to spatially variable soil properties.

Keywords: piled foundation, soil-structure interaction, spatial variability, probabilistic analyses, random field modeling

*Corresponding author
Email address: andy.yf.leung@polyu.edu.hk (Y.F. Leung)

1. Introduction

The designs of large pile groups or piled rafts are often controlled by differential settlements, which may cause distortion or tilting of the structure. However, in previous studies of probabilistic analyses of piles and pile groups [e.g., 1, 2, 3, 4, 5, 6, 7], there have been limited discussions on the uncertainties associated with these aspects of piled foundation response, and their inter-relationship with spatial variability of soil properties and influence of superstructure. This may be partly attributed to the complex interaction effects in the system. Simulating all superstructure elements, foundation components and subsurface domain using a single finite element model involves substantial computational demands. The problem is exacerbated for probabilistic assessments that require a large number of analyses for typical Monte Carlo approaches.

This note proposes an efficient approach to circumvent these issues, which enables the impacts of three-dimensional soil variability and superstructure stiffening effects to be considered in probabilistic analyses of large piled foundations. To reduce computational demands, stiffness components of the spatially variable subsurface domain and superstructure are evaluated separately through matrix condensation techniques, and then incorporated with the foundation model. Two piled raft case studies are presented to show that the probabilistic approach may reveal deformation mechanisms in large foundations that cannot be captured by the conventional deterministic approach.

2. Response model for pile groups in spatially variable soils

Fig. 1 illustrates the concept of matrix condensation applied to both the superstructure and foundation soil with spatial variations, which avoids the excessive computational demands associated with modeling the entire system in a single numerical model. The pile group analysis approach is conceptually similar to that by [8], except for the modeling of spatially variable soil domain. The piles and the cap (or raft if in touch with foundation soil) are discretized into segments specified by nodes. In the case of linear-elasticity, the displacements, $\boldsymbol{u}$, is given by:

$$\left(\mathbf{K}^{p} + \mathbf{K}^{r} + \mathbf{K}^{s}\right)\boldsymbol{u} = \boldsymbol{p}^{w} + \boldsymbol{p}^{g} = \boldsymbol{p}^{w} - \mathbf{F}^{-1}\boldsymbol{u} \tag{1}$$

where $\mathbf{K}^p$ = stiffness matrix of piles modeled as one-dimensional beam elements; $\mathbf{K}^r$ = stiffness matrix of pile cap, modeled as four-node thin plate elements; $\mathbf{K}^s$ = condensed structure matrix; $\boldsymbol{p}^w$ = loading from superstructure; $\boldsymbol{p}^g$ = ground reaction forces acting on foundation elements, which are equal and opposite to the pile forces on soil, represented through the soil flexibility matrix $\mathbf{F}$. In this study, only the vertical displacements are considered.

The condensed matrix $\mathbf{K}^s$ represents the rigidity of superstructure against differential displacements at its connections to the foundation, which may be columns or walls modeled as discrete supports. Its components K^s_{ij} can be obtained through a finite element model of the superstructure, where a unit displacement is applied at column j while fixing the other supports, and reaction forces at each support i are then extracted. For a superstructure with n supports, this procedure is repeated by n times to construct a $n \times n$ matrix [8]. To model soil nonlinearity, $\boldsymbol{u}$ consists of a continuum component and a plastic slip component ($\boldsymbol{u}^{ip}$), in which case Eq. (1) becomes [9, 10]:

$$\begin{aligned} & \left(\mathbf{K}^s + \mathbf{K}^p + \mathbf{K}^r + \mathbf{K}^*\right)\boldsymbol{u} = \boldsymbol{p}^w + \mathbf{K}^*\mathbf{F}^*\langle \boldsymbol{p}^{in}\rangle + \mathbf{K}^*\boldsymbol{u}^{ip} \\ \text{where} \quad & \langle \boldsymbol{p}^{in}\rangle_i = \min\left\{\left[\boldsymbol{p}^w - \left(\mathbf{K}^s + \mathbf{K}^p + \mathbf{K}^r\right)\boldsymbol{u}\right]_i, f_{lim}\right\} \end{aligned} \tag{2}$$

and $\mathbf{K}^*$ = local soil stiffness matrix and is diagonal ($K^*_{ii} = 1/F_{ii}$), $\mathbf{F}^*$ = soil flexibility matrix without the main diagonal, and f_{lim} = limit force at the nodes, evaluated based on the raft bearing capacity or pile shaft or base resistance; $\boldsymbol{u}^{ip}$ = plastic displacements when the soil-pile interface force exceeds f_{lim}, and Eq. (2) can be solved by an iterative process [10]. Derivation from Eq. (1) to Eq. (2), and its validation for deterministic analysis are presented in [8].

The objective of this study is to incorporate spatial variability of soil properties into analyses of large pile groups. For this purpose, formulation of soil flexibility matrix, $\mathbf{F}$, is modified here. This matrix represents the pile-soil-pile interaction effects and is often evaluated using elastic solutions [11, 12]. There is, however, no closed-form solution for three-dimensional random fields of spatially variable modulus. The finite element method is therefore adopted. The procedure is essentially a matrix condensation technique: when a unit force is applied at pile node location j, displacements

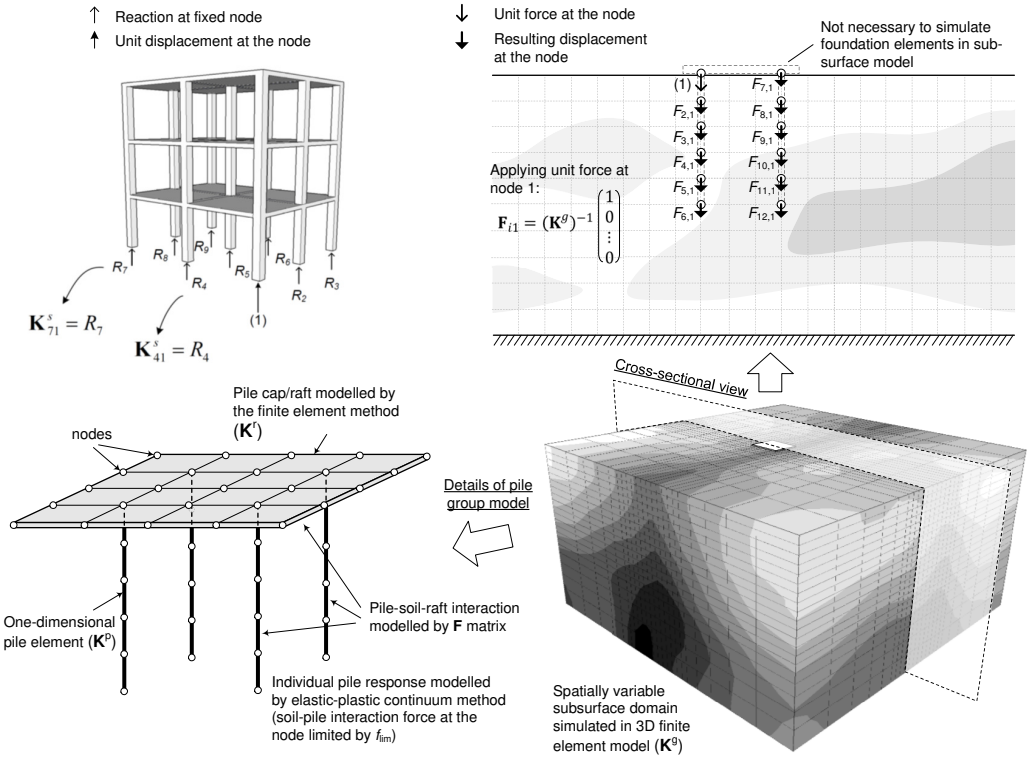

Figure 1: Formulation of probabilistic pile group analysis approach

at other pile node locations are extracted as a vector $\{F_{1j}, F_{2j}, F_{3j}, \ldots, F_{ij}\}^T$, and this is repeated at all pile nodes to obtain the complete $\mathbf{F}$ matrix. In a probabilistic assessment, each random field realization is associated with a different $\mathbf{F}$ matrix.

In the proposed approach (Fig. 1), the superstructure stiffness ($\mathbf{K}^s$) and subsurface soil flexibility ($\mathbf{F}$) matrices are evaluated separately by matrix condensation technique, and then coupled to the stiffness of foundation elements through Eq. (2). Therefore, it is not necessary to simulate the piles or raft in the three-dimensional subsurface model, which is streamlined to evaluate only the pile-to-pile and pile-to-raft interaction effects. A finite element program is written in this study for such purpose, adopting eight-node hexahedral elements with two Gauss points in each direction, i.e., 8 Gauss points per element. Each element involves a different stiffness matrix, $\mathbf{K}^e$, due to differences in both element geometries and deformation moduli. The global subsurface stiffness matrix, $\mathbf{K}^g$, is then assembled for evaluation of $\mathbf{F}$. As discussed, nonlinearity of pile behavior is

modeled through the slip displacement $\boldsymbol{u}^{ip}$, by limiting f_{lim} at soil-pile interface, while interaction effects between the piles are modeled as linear-elastic. This is consistent with [13], who stated that soil nonlinearity is confined to a narrow zone around the pile, and soil response remains essentially elastic outside this zone. This phenomenon is further discussed in [9, 14, 15, 16, 17].

3. Probabilistic analyses of pile groups with rigid or flexible caps

In this study, the soil properties are represented as a combination of the trend ($\boldsymbol{t}$) and residuals ($\boldsymbol{e}$). The residuals (or deviations from trend) are often observed to be correlated spatially [18, 19], with their uncertainties represented by the spatial covariance matrix $\mathbf{V}$, which can be factored as $\mathbf{V} = \sigma^2\mathbf{R}$, where σ^2 = variance of $\boldsymbol{e}$ across the domain; $\mathbf{R}$ = spatial correlation matrix, with components R_{ij} represented by a squared exponential function describing correlation of parameters at various locations:

$$R_{ij} = \exp\left[-\frac{(x_i - x_j)^2}{\theta_x^2} - \frac{(y_i - y_j)^2}{\theta_y^2} - \frac{(z_i - z_j)^2}{\theta_z^2}\right] \tag{3}$$

where x, y, z = Cartesian coordinates at locations i and j; θ_x, θ_y, θ_z = autocovariance distances (or $\theta_{\ln x}$, $\theta_{\ln y}$ and $\theta_{\ln z}$ for lognormally distributed properties). Probabilistic analyses are performed using the approach developed by [20], which combines the stratified sampling method called Latin Hypercube Sampling with Dependence (LHSD) [21] with surrogate modeling technique of polynomial chaos expansion (PCE) [22, 23, 24, 25], briefly described in the appendix. LHSD ensures the spatially correlated random variables are evenly spread across the multi-dimensional sampling domain, while PCE effectively approximates the system response and reduces the computational demands of probabilistic assessment. The derivation and implementation of the LHSD-PCE approach can be found in [20], where its effectiveness in handling large numbers of random variables for random field modeling is illustrated through shallow footing and slope stability problems.

The proposed approach is first validated through comparisons with results by [2], who analyzed the settlement uncertainty of pile groups with a rigid cap, embedded in linear-elastic soils with modulus varying in the vertical (z) direction. Normally distributed soil properties were considered

by [2], and the corresponding coefficient of variation (CV) in settlements (CV_m) is presented as a ratio of CV in Young's modulus (CV_E). The same pile geometry (length-to-diameter ratio, L/D) and properties (pile to soil modulus ratio, E_p/E_s) are analyzed in this study, and Fig. 2 shows that the two approaches generally produce very similar results. At higher values of θ_z (comparable to L), CV_m estimated by the proposed approach is larger than that by [2]. This may be attributed to the first-order second-moment approach they adopted, which involves truncation of higher order variation terms. The effect is more apparent when the model response involves large variability.

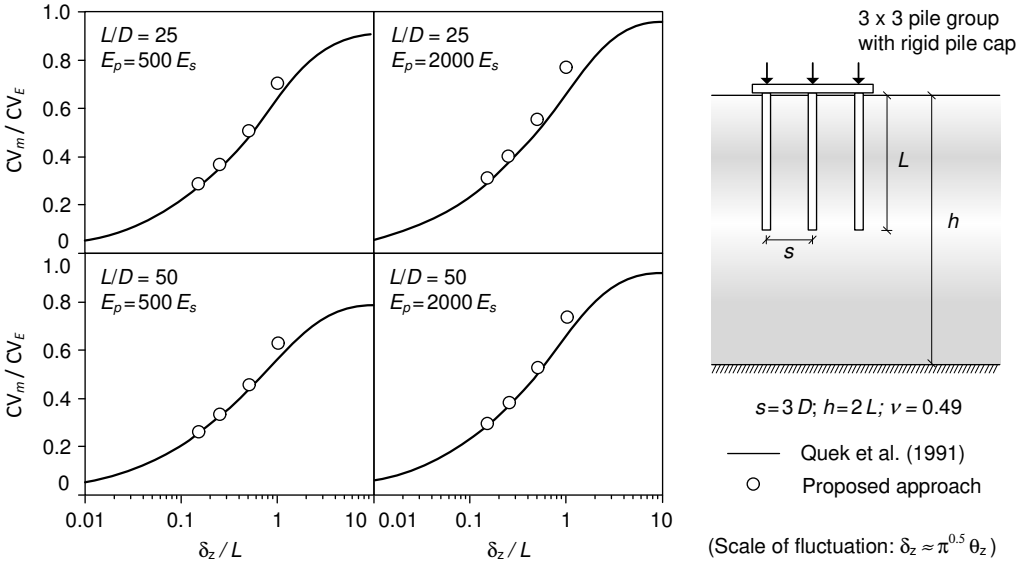

Figure 2: Probabilistic analyses of 3×3 pile group with rigid pile cap

For pile groups with caps of various thickness, the design concern becomes the differential settlements (Δ). A recent study [7] investigated the differential settlements between two piles installed in spatially variable soils, and suggested that Δ is largest when θ is approximately equal to the spacing (s) between the piles. In their study, the soil is elastic and the spatial variation of Young's modulus is isotropic ($\theta_{\ln x} = \theta_{\ln y} = \theta_{\ln z}$). This two-pile scenario is also analyzed using the proposed approach for comparison with their simplified formula, where CV_E values of 0.3 and 0.5 are adopted and θ varies from $0.5s$ to $3s$ (Fig. 3). The mean and standard deviations of Δ are normalized by deterministic estimates (assuming homogeneous soil) of single pile settlement. In

general, the two approaches produce similar results, and the worst case scenario with maximum Δ occurs when θ is about 1 to 2s.

This study also investigates 3×3 and 5×5 pile groups with a 'flexible' cap, founded on elastic soils with anisotropic spatial variation patterns. Various combinations of $\theta_{\ln z}$ and $\theta_{\ln x}(=\theta_{\ln y})$ are studied, with $\theta_{\ln z}$ ranging from $0.15L$ to $1L$, and $\theta_{\ln x}$ equals $0.5B$, $1B$ (B =width of foundation) or ∞ (a large value exceeding the size of domain). Fig. 4 shows the coefficients of variation in average settlement (CV_m) and differential settlement (CV_Δ), with the Δ defined herein as the difference between maximum and minimum settlements across the pile group. CV_E values of 0.25 or 0.5 are adopted. While the results appear to line up for normalized $\mathrm{CV}_m/\mathrm{CV}_E$ (Figs. 4a and c), wider ranges are noted for $\mathrm{CV}_\Delta/\mathrm{CV}_E$ (Fig. 4b and d), especially for small values of $\theta_{\ln x}$. This 'band' arises mainly due to the fact that Δ is not only a function of E_s. It is also heavily influenced by geometry of the foundation, pile configurations and $\theta_{\ln x}$, causing the uncertainty in Δ to increase at a lower rate than uncertainty in E_s. On the contrary, the average settlement is largely dominated by E_s, so the rates of change in CV_m and CV_E are similar and a 'band' does not appear.

While CV_m increases with $\theta_{\ln x}$, CV_Δ does not display a monotonic trend with $\theta_{\ln x}$. CV_Δ is smallest in a layered soil profile with $\theta_{\ln x}=\infty$, and increases as the soil involves higher variability in horizontal directions. When the spatial variation features match with the foundation geometry, the impacts on differential settlements can be magnified, as the settlement trough (i.e., settlement profile across the horizontal dimensions) can be distorted by sudden changes in E_s along lateral directions. Some combinations of soil variability features ($\theta_{\ln x}$) and foundation width (B) can lead to the value of $\mathrm{CV}_\Delta/\mathrm{CV}_E$ exceeding one. For a 5×5 pile group, the maximum CV_Δ occurs at $\theta_{\ln x}=B$, while 3×3 pile group may demonstrate largest CV_Δ when $\theta_{\ln x}=B$ or $0.5B$, depending on the spatial variability features. As $\theta_{\ln x}$ decreases further, the variations in modulus become 'averaged out' within foundation footprint and CV_Δ decreases. This is a vivid example of the phenomenon that the worst case scenario often lies between assumptions of perfect spatial correlation ($\theta=\infty$) and no spatial correlation ($\theta=0$) between soil properties.

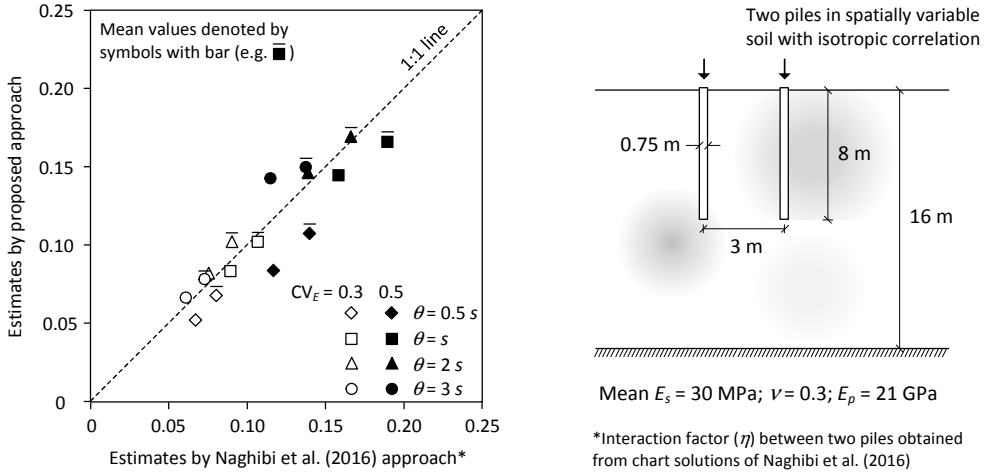

Figure 3: Mean and standard deviation of differential settlements normalized by deterministic single pile settlement, estimated by the proposed approach and Naghibi et al. (2016) simplified formula

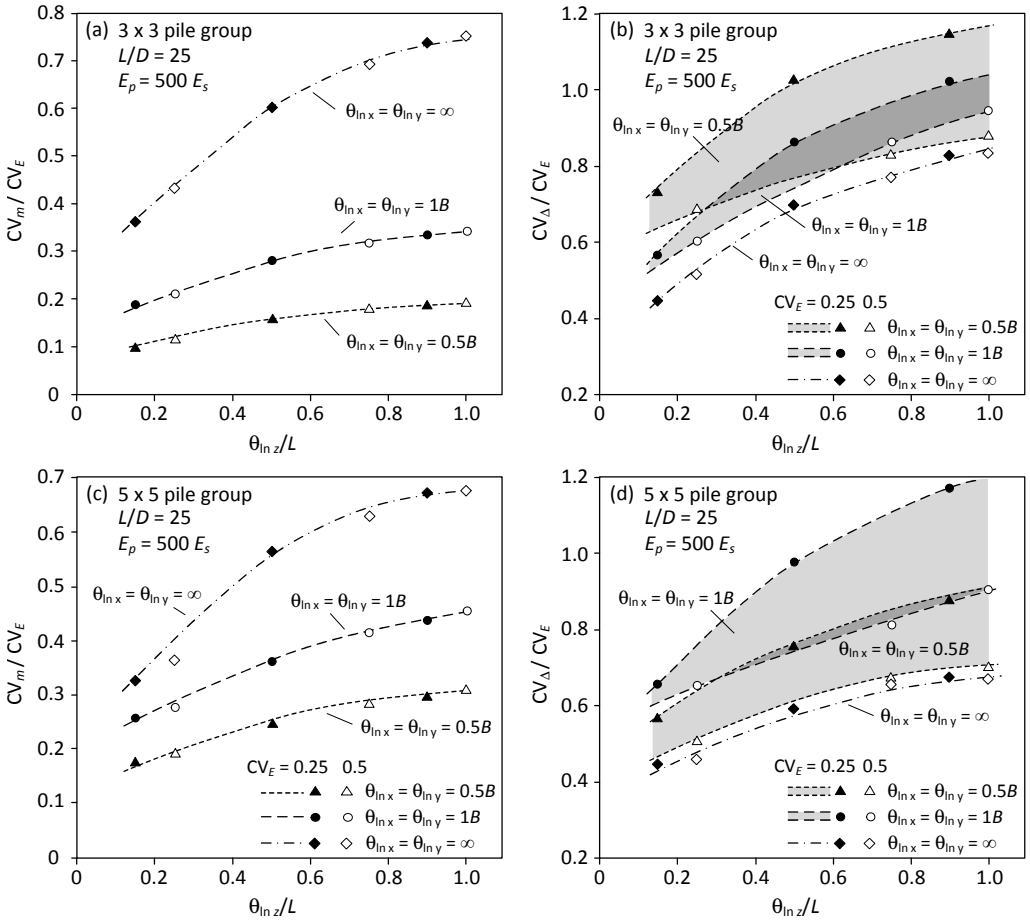

Figure 4: Probabilistic analyses of 3×3 and 5×5 pile groups with flexible pile cap

4. Case study 1: Hyde Park Cavalry Barracks tower foundation, London

Two piled raft case studies are re-analyzed using the proposed approach, to illustrate the significance of probabilistic assessments and potentials of their implementation in foundation designs. The first case involves the Hyde Park Cavalry Barracks (HPCB) tower in London, UK, with the foundation and superstructure details reported in [26] and [8]. The tower is 90 m tall with 31 storeys and a two-storey basement, with the structural floor plan consisting of core walls running across the building footprint. It is founded on a 1.52-m thick raft supported by 51 under-reamed piles, each with length of 24.8 m, shaft diameter of 0.91 m and base diameter of 2.44 m. The piled raft is embedded in London Clay, with groundwater level approximately 4 m below the surface. Based on findings by [26], the following relationships are adopted as trends of Young's modulus (t_E in MPa) and undrained shear strength (t_{cu} in kPa) of London Clay at the site:

$$t_E = 27 + 3.9 z_{clay} \tag{4}$$

$$t_{cu} = 100 + 11 z_{clay} \tag{5}$$

where z_{clay} = depth (in m) measured from top of the clay surface, 5 m below ground surface. The pile shaft and base resistance (f_{lim}) are estimated by the total stress method, adopting $\alpha = 0.5$.

In this study, the coefficient of variation for E_s and c_u is assumed to be 40%, which broadly agrees with the data in [26], and the two properties are assumed to be lognormally distributed with perfectly-correlated residuals (cross-correlation coefficient equals 1 between E_s and c_u). $\theta_{\ln x}$ and $\theta_{\ln y}$ are assumed to be 26 m, which is equal to the foundation width; $\theta_{\ln z}$ is assumed to be half of the pile length. These are also comparable to typical values reported in various studies [27, 28]. In the numerical analyses, each pile is discretized into ten 2.5-m long elements. The finite element mesh for evaluation of $\mathbf{F}$ matrix consists of about 8700 elements, with lateral boundaries located more than 40 m away from the foundation edges. Fig. 5 shows two realizations of subsurface spatial variations of E_s, with linearly increasing trend described by Eq. (4) and spatially correlated residuals. The mesh is finer near the piles, with element sizes gradually increasing from 1.4 m×1.6 m×2.5 m around

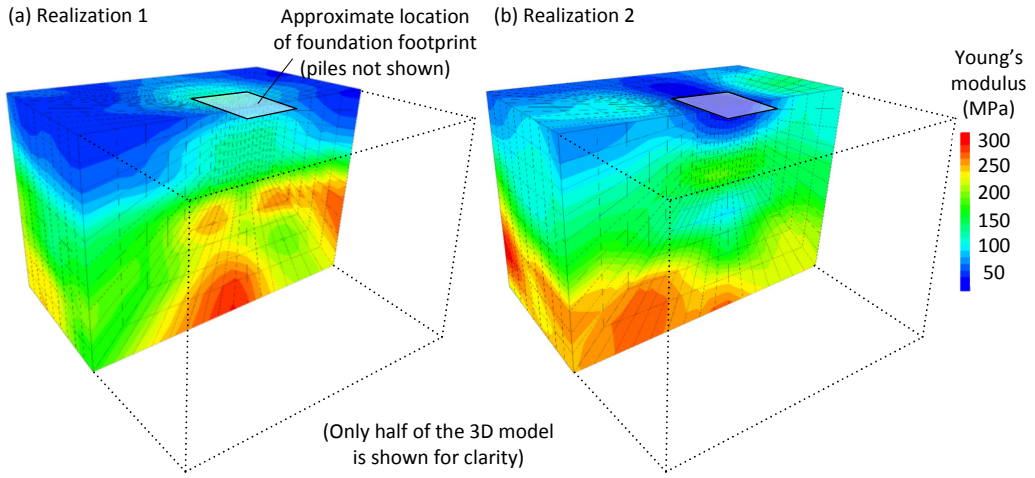

Figure 5: Two example realizations of the subsurface domain for HPCB foundation

the piles to approximately 6.5 m×6.5 m×9 m (elongated, inclined element) near the boundaries of model domain, far away from the piles. The subsurface models do not involve piles or superstructure elements, as their stiffness matrices are evaluated separately.

With these spatial correlation parameters, 1,000 realizations are simulated by LHSD. The simulated E_s and c_u values are mapped directly to the midpoint of each element, as local averaging produces negligible variance reduction (less than 1%) for elements near the piles. Each soil profile realization leads to a corresponding $\mathbf{F}$ matrix, which is then combined with the pile and raft stiffness, and the system responses are analyzed by Eq. (2). Two separate scenarios are analyzed, with and without consideration of $\mathbf{K}^s$ matrix that represent stiffening effects of the superstructure. In both scenarios, the PCE coefficients are determined through the sparse PCE procedure, utilizing the analysis results of 1,000 realizations. The probability densities for piled raft response are then generated through 10,000 evaluations of the surrogate model.

The measured center settlement and diagonal differential settlements are 21 mm and 6.6 mm, respectively [26]. The pile forces at two instrumented piles are presented in this study, where the measured forces are 3.4 MN at the center pile, and 2.9 MN at the pile denoted as P2 by [26] and [8]. These are compared with the probability density obtained from the probabilistic

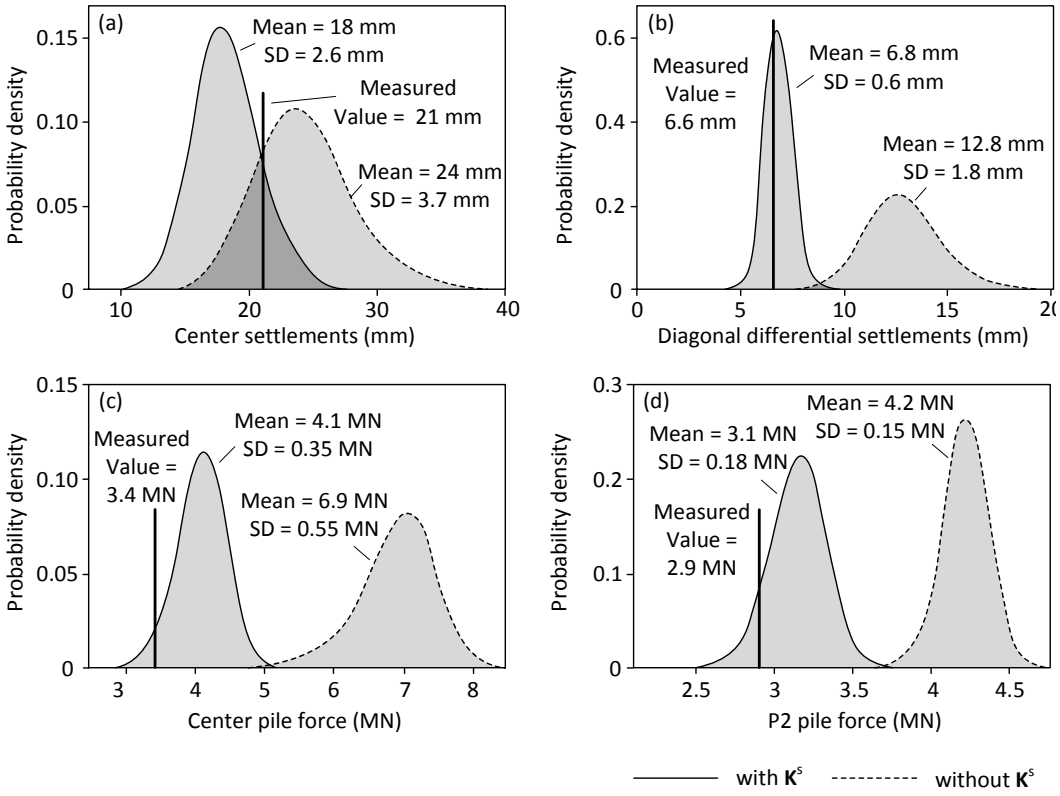

Figure 6: Probabilistic analyses of HPCB foundation with and without considering superstructure stiffness: (a) center settlement; (b) diagonal differential settlements; (c) force at center pile; (d) force at pile P2

analyses in Fig. 6, which represent the probable ranges of piled raft response considering soil spatial variations. In cases where the measured response lies outside this range, the discrepancies between predicted and measured behaviors cannot be explained by soil variability alone. The results from probabilistic analyses incorporating $\mathbf{K}^s$ generally agree with the measurements, which are broadly covered by the mean estimate ± 1 standard deviation (SD), except for the center pile force, with the measured value equal to mean estimate minus 2 SD. On the contrary, ignoring $\mathbf{K}^s$ in the analyses leads to substantial discrepancies from the measurements, particularly for differential settlements and pile force estimates. Such discrepancies cannot be 'enveloped' by geotechnical variability, as the foundation response is fundamentally different under the influence of a stiff superstructure.

This illustrates the capabilities of the probabilistic approach in providing prediction ranges of piled raft response considering soil spatial variability, and also highlights the importance of proper considerations of structure interactions, especially when the raft is flexible (1.52 m thick) compared to the superstructure, which involves a number of stiff shear walls in this case.

5. Case study 2: Westendstrasse 1 tower foundation, Frankfurt

The second case involves the Westendstrasse 1 tower in Frankfurt, with information on the tower and its foundation reported in [29, 30, 31]. The tower is 208 m tall with 51 storeys, adjacent to a 60-m tall side building supported on a raft, with the two buildings separated by settlement joints. The tower is supported by a piled raft with the raft founded at a depth of 14.5 m. The raft footprint is parallelogram in shape, and approximated as rectangular in subsequent analyses. The foundation consisted of 40 piles with diameter of 1.3 m and length of 30 m, and pile load measurements are available for six piles. The central part of the raft is 4.5 m thick, with thickness reducing to 3 m at the edges. Details of the superstructure layout of the tower are not available, but it is unlikely to have substantial influence on the foundation response considering the raft thickness. The effective structural load is 957 MN. Due to the lack of information on the superstructure column layout, the building load is uniformly distributed as a vertical stress of 338 kPa, which is consistent with the assumptions of [31].

The piled raft is embedded in the Frankfurt Clay stratum which is highly heterogeneous [30, 31]. The depth to the stiff Frankfurt limestone is uncertain, and is assumed to be 70 m below the surface of Frankfurt Clay. There are some discrepancies over its stiffness reported in different studies [29, 31]. Considering the previous investigations, the following relationships are adopted for the trend values of Young's modulus (in MPa) and undrained shear strength (in kPa) of Frankfurt clay:

$$t_E = \begin{cases} 60 & \text{if } z_{clay} \leq 25 \\ 60 + 2.45 z_{clay} & \text{if } z_{clay} > 25 \end{cases} \tag{6}$$

$$t_{cu} = 127 + 3.93 z_{clay} \tag{7}$$

which lies between the values suggested by [29] and [31]. The total stress method is adopted for estimation of pile shaft resistance, with α assumed to be 0.45.

Variability of the Frankfurt clay is known to be significant, with coefficients of variation for shear strength parameters as high as 50% [32]. This CV value is adopted for both Young's modulus and undrained shear strength, assumed to be lognormally distributed with perfectly correlated residuals. The autocovariance distances at the site are not reported in the literature. Two sets of analyses are therefore performed. In the first modeling scenario, $\theta_{\ln x}$ and $\theta_{\ln y}$ are assumed to be equal to width of the raft, i.e., 47 m. $\theta_{\ln z}$ is assumed to be 15 m, which equals half of the pile length. In the second scenario, 'layered' soil profiles are generated with $\theta_{\ln x} = \theta_{\ln y} = \infty$, and $\theta_{\ln z} = 7.5$ m. Each pile is discretized into ten elements, and the finite element mesh for evaluation of $\mathbf{F}$ matrix consists of about 9460 elements. Lateral boundaries of the model are more than 70 m away from the foundation edges. 1,000 realizations are generated for each scenario, and analyzed by Eq. (2) to construct the PCE. After determining the PCE coefficients, probability density for various aspects of the response are obtained with 10,000 evaluations of the surrogate model.

Fig. 7 shows the probability densities for center settlement, minimum and maximum pile forces, compared with the measured data. The measured center settlement was 110 mm, and the maximum and minimum pile forces are 16.6 and 12.0 MN, respectively. Foundation tilt of $\omega = 1/1600$ was also observed, while Fig. 7b shows the probability density of $\log(1/\omega)$. In general, the predicted mean values are close to the measured response. More importantly, probabilistic analyses allow prediction of the potential tilting due to spatial variations in soils, when $\theta_{\ln x}$ and $\theta_{\ln y}$ are comparable to the foundation dimensions (first scenario). For example, Figs. 7(e) and (f) show the settlement profiles estimated for two realizations (from the first scenario) with notable tilt. On the contrary, 'layered' soil profiles predict much smaller foundation tilt, which arise solely due to asymmetry of the pile configuration. Predicted pile force variations are also smaller in the second modeling scenario.

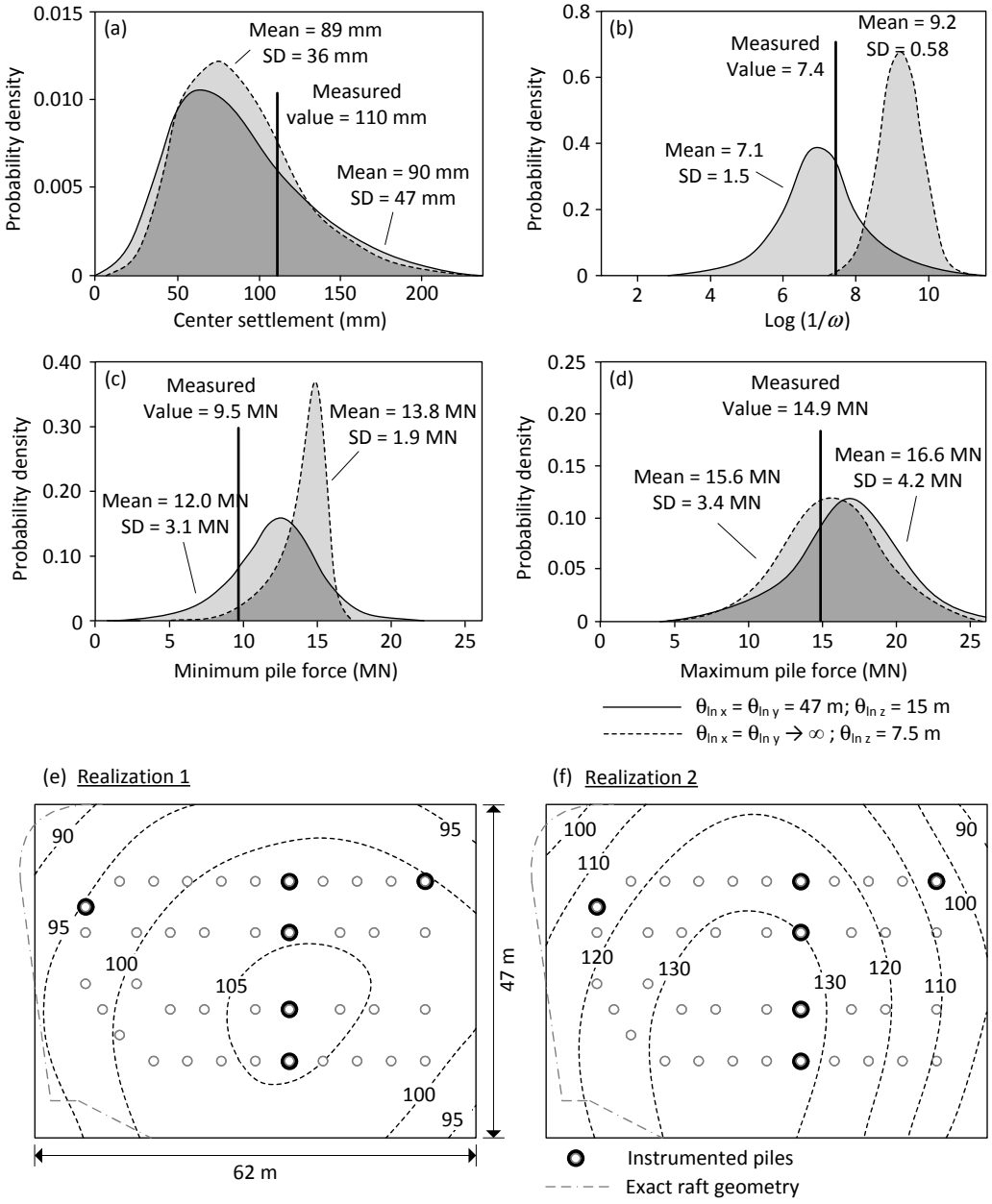

Figure 7: Probabilistic analyses of Westendstrasse 1 foundation: (a) center settlement; (b) tilting; (c) maximum pile force; and (d) minimum pile force; (e,f) Settlements (in mm) for two example realizations with notable tilting

6. Conclusion

This note introduces an approach for probabilistic analyses of large pile groups and piled rafts founded on soils with spatially correlated properties varying in three dimensions. The method

involves condensation of stiffness matrices representing contributions from the superstructure and spatially variable subsurface domain. This is implemented with the LHSD-PCE approach, which allows efficient probabilistic assessments for complex soil-structure interaction problems involving different patterns of soil variability. For example, 3×3 and 5×5 pile group analyses showed that the critical scenarios for differential settlements involve the horizontal autocovariance distance being comparable to the foundation dimensions. The enhanced computational efficiency also makes the approach suitable for practical large-scale foundation projects. The two case studies illustrate the importance of stiffening effects of the superstructure, and the capabilities of the approach in estimating potentials of tiling response that cannot be captured by deterministic analyses.

Assumptions have been made regarding the spatial correlation features in the two case studies. These are necessary due to the lack of published data for site-specific characterization of spatial variability. Such information, if available, will improve the random field models and lead to better representations of the site conditions.

Appendix: surrogate modeling by PCE

The concept of PCE technique involves the approximation of system response g, which may be foundation settlements or internal forces on the piles, by an analytical equation [22, 25, 33]:

$$g(\boldsymbol{\xi}) = \sum_{\beta=0}^{P-1} a_\beta \Psi_\beta; \quad \text{where } P = \frac{(M+2)!}{M!2!} \tag{8}$$

where a_β are PCE coefficients; P is the number of coefficients; Ψ_β are polynomials constructed by $\boldsymbol{\xi}$, which is a $(M \times 1)$ vector of independent standard normal variables. $\boldsymbol{\xi}$ is related to the residuals ($\boldsymbol{e}$) of soil properties by the linear transformation: $\boldsymbol{e} = \mathbf{H}\boldsymbol{\Lambda}^{1/2}\boldsymbol{\xi}$, with $\mathbf{H}$ and $\boldsymbol{\Lambda}$ obtained from spectral decomposition of the spatial correlation matrix: $\mathbf{R} = \mathbf{H}\boldsymbol{\Lambda}\mathbf{H}^T$. Originally, M equals to the length of $\boldsymbol{e}$, but M can be reduced significantly by only keeping the $\boldsymbol{\xi}$ components that contribute to most (e.g., 95%) of the variance in $\boldsymbol{e}$ [20].

The coefficients a_β are computed through a regression approach [23], which involves simulation

of n sets of $\boldsymbol{\xi}$ $(\boldsymbol{\xi}^{(1)}, \boldsymbol{\xi}^{(2)}, \ldots, \boldsymbol{\xi}^{(n)})$. For example, $n = 1000$ for the two presented case studies. $\boldsymbol{\xi}$ are generated using LHSD method, which is an efficient stratified sampling scheme. Readers are referred to [20] for the details of implementation of LHSD. For each of the n realizations, a different $\mathbf{F}$ matrix is obtained, followed by the foundation analyses through Eq. (2), resulting in n system responses $(g^{(1)}, g^{(2)}, \ldots, g^{(n)})$. The a_β coefficients can be grouped as a vector $\hat{\boldsymbol{a}}$, and estimated as the least square estimator of the regression analysis:

$$\begin{aligned} & \hat{\boldsymbol{a}} = \left(\boldsymbol{\eta}^T \boldsymbol{\eta}\right)^{-1} \boldsymbol{\eta}^T \boldsymbol{\Gamma} \\ \text{where} \quad & \boldsymbol{\eta}_{ij} = \Psi_{j-1}(\boldsymbol{\xi}^{(i)}) \qquad i = 1, 2, \ldots, n; \quad j = 1, 2, \ldots, P \\ & \boldsymbol{\Gamma} = \left\{ g^{(1)}, g^{(2)}, \ldots, g^{(n)} \right\}^T \end{aligned} \tag{9}$$

With a_β determined, the probability density of $g(\boldsymbol{\xi})$ can be constructed by evaluating Eq. (8) directly with a large number (much larger than n) of simulated $\boldsymbol{\xi}$. This step is efficient as Eq. (8) approximates the response and does not involve additional geotechnical analyses.

Acknowledgement

The work presented in this note is financially supported by the Research Grants Council of the Hong Kong Special Administrative Region (Project No. 25201214).

References

[1] K. K. Phoon, S. T. Quek, Y. K. Chow, S. L. Lee, Reliability analysis of pile settlement, J. Geotech. Engrg. 116 (11) (1990) 1717–1734.

[2] S. T. Quek, K. K. Phoon, Y. K. Chow, Pile group settlement: A probabilistic approach, Int. J. Numer. Anal. Methods Geomech. 15 (11) (1991) 817–832.

[3] S. T. Quek, Y. K. Chow, K. K. Phoon, Further contributions to reliability-based pile-settlement analysis, J. Geotech. Engrg. 118 (5) (1992) 726–741.

[4] G. A. Fenton, D. V. Griffiths, Reliability-based deep foundation design, in: ASCE GSP 170 Probabilistic Applications in Geotechnical Engineering, 2007, p. 10.1061/40914(233)1.

[5] Y. Wang, S.-K. Au, F. H. Kulhawy, Expanded reliability-based design approach for drilled shafts, J. Geotech. Geoenviron. Eng. 137 (2) (2011) 140–149.

[6] F. Naghibi, G. A. Fenton, D. V. Griffiths, Serviceability limit state design of deep foundations, Géotechnique 64 (10) (2014) 787–799.

[7] F. Naghibi, G. A. Fenton, D. V. Griffiths, Probabilistic considerations for the design of deep foundations against excessive differential settlement, Can. Geotech. J. 53 (7) (2016) 1167–1175.

[8] Y. F. Leung, A. Klar, K. Soga, N. A. Hoult, Superstructure-foundation interaction in multi-objective optimization of pile groups considering settlement response, Can. Geotech. J. 54 (10) (2017) 1408–1420.

[9] Y. F. Leung, K. Soga, B. M. Lehane, A. Klar, Role of linear elasticity in pile group analysis and load test interpretation, J. Geotech. Geoenviron. Eng. 136 (2010) 1686–1694.

[10] A. Klar, T. E. B. Vorster, K. Soga, R. J. Mair, Elastoplastic solution for soil-pipe-tunnel interaction, J. Geotech. Geoenviron. Eng. 133 (2007) 782–792.

[11] R. D. Mindlin, Force at a point in the interior of a semi-infinite solid, Physics 7 (1936) 195–202.

[12] K. S. Chan, P. Karasudhi, S. L. Lee, Force at a point in the interior of a layered elastic half space, International Journal of Solids Structures 10 (1974) 1179–1199.

[13] Y. K. Chow, Analysis of vertically loaded pile groups, Int. J. Numer. Anal. Methods Geomech. 10 (1) (1986) 59–72.

[14] V. Caputo, C. Viggiani, Pile foundation analysis: Simple approach to nonlinearity effects, Rivista Italiana di Geotecnica 18 (2) (1984) 32–51.

[15] H. G. Poulos, Pile behaviour - theory and application, Géotechnique 39 (3) (1989) 365–415.

[16] K. M. Lee, Z. R. Xiao, Simplified nonlinear approach for pile group settlement analysis in multilayered soils, Can. Geotech. J. 38 (5) (2001) 1063–1080.

[17] A. Mandolini, G. Russo, C. Viggiani, Pile foundations: experimental investigations, analysis and design, Proc., 16th Conf. on Soil Mech. & Geotech. Engrg (2005) 177–213.

[18] D. J. DeGroot, G. B. Baecher, Estimating autocovariance of in-situ soil properties, J. Geotech. Engrg. 10.1061/(ASCE)0733-9410(1993)119:1(147) (1993) 147–166.

[19] D. J. DeGroot, Analyzing spatial variability of in situ soil properties, in: Uncertainty in the Geologic Environment: From Theory to Practice, Vol. 1, 1996, pp. 210–238.

[20] M. K. Lo, Y. F. Leung, Probabilistic analyses of slopes and footings with spatially variable soils considering cross-correlation and conditioned random fields, J. Geotech. Geoenviron. Eng. 10.1061/(ASCE)GT.1943-5606.0001720 (2017) 04017044.

[21] N. Packham, W. M. Schmidt, Latin hypercube sampling with dependence and applications in finance, Journal of Computational Finance 13 (3) (2010) 81–111.

[22] R. G. Ghanem, P. D. Spanos, Stochastic Finite Element: A Spectral Approach, Springer, New York, 1991.

[23] G. Blatman, B. Sudret, An adaptive algorithm to build up sparse polynomial chaos expansions for stochastic finite element analysis, Probab. Engrg. Mech. 25 (2010) 183–197.

[24] G.-Y. Sheu, Prediction of probabilistic settlements via spectral stochastic meshless local petrovgalerkin method, Computers and Geotechnics 38 (4) (2011) 407 – 415.

[25] T. Al-Bittar, A.-H. Soubra, Probabilistic analysis of strip footings resting on spatially varying soils and subjected to vertical or inclined loads, J. Geotech. Geoenviron. Eng. 10.1061/(ASCE)GT.1943-5606.0001046 (2014) 04013043.

[26] J. A. Hooper, Observations on the behaviour of a piled-raft foundation on London clay, Proc. Instn. Civ. Engrs. 55 (1973) 855–877.

[27] K. K. Phoon, F. H. Kulhawy, Characterization of geotechnical variability, Can. Geotech. J. 36 (4) (1999) 612–624.

[28] W. F. Liu, Y. F. Leung, Characterising three-dimensional anisotropic spatial correlation of soil properties through *in situ* test results, Géotechnique (in press).

[29] E. Franke, Y. El-Mossallamy, P. Wittmann, Calculation methods for raft foundations in Germany, Design applications of raft foundations (2000) 283–322.

[30] R. Katzenbach, U. Arslan, C. Moormann, Piled raft foundation projects in Germany, Design applications of raft foundations (2000) 323–391.

[31] O. Reul, M. F. Randolph, Piled rafts in overconsolidated clay: comparison of in situ measurements and numerical analyses, Géotechnique 53 (3) (2003) 301–315.

[32] C. Russelli, P. A. Vermeer, Probabilistic methods applied to geotechnical engineering, in: Proceedings of the 2nd Int. Workshop of Young Doctors in Geomechanics, 2005, pp. 1–4.

[33] H.-Q. Yang, L. Zhang, D.-Q. Li, Efficient method for probabilistic estimation of spatially varied hydraulic properties in a soil slope based on field responses: A Bayesian approach, Computers and Geotechnics (2018) in press.